C.4b.1-JPACR2018.pdf

By Risfidian Mohadi

WORD COUNT	5577	TIME SUBMITTED	22-JAN-2022 10:01AM
		PAPER ID	81672161

DOI: 10.21776/ub.jpacr.2018.007.02.351 *J. Pure App. Chem. Res.*, **2018**, 7(2), 79-93
1 May 2018

Thermal Activated of Indonesian Bentonite as A Low-Cost Adsorbent for Procion Red Removal from Aqueous Solution

Tarmizi Taher[1], Dedi Rohendi[2], Risfidian Mohadi[2], Aldes Lesbani[1,2*]

[1] Department of Environmental Science, Graduate School, Universitas Sriwijaya, Jl. Padang Selasa, No. 524, Ilir Barat I, Palembang, Indonesia

[2] Department of Chemistry, Faculty of Mathematics and Natural Science, Universitas Sriwijaya, Jl. Palembang-Prabumulih, Km. 32, Ogan Ilir, Indonesia

[*]Corresponding email: aldeslesbani@pps.unsri.ac.id

Received 29 July 2017; Accepted 8 January 2018

ABSTRACT

Abundant and inexpensive Indonesian natural bentonite was activated by thermal activation at 500°C for removal of procion red dye as one of the most used synthetic dye in the traditional songket fabric production around Palembang city. Activated bentonite product was characterized by FT-IR, XRD, and thermal analysis. The adsorption process was conducted in batch adsorption system by applying various adsorption parameter condition including, initial pH condition, contact time, and initial dye concentration. The activated bentonite characterization indicates that during the activation process, the structure of the original bentonite was not changed significantly and the result of the thermal analysis revealed that thermal activation at 500°C was draining the water content without destructing the silica-alumina framework of bentonite. The adsorption kinetics study shows that the procion red adsorption into the activated bentonite follows the pseudo-second order kinetic model. The isotherm adsorption study revealed that procion red adsorption into activated bentonite adapted the Langmuir adsorption isotherm.

Key word: Indonesian bentonite, adsorption, procion red

INTRODUCTION

The effluent of modern and conventional industry such as textile, food, plastic, and cosmetic contains various of chemical compounds like dyes and pigment. The disposal of these effluents directly onto the environment will cause the dangerous water pollution[1]. Most of the dye used in the commercial industry contains complex organic molecules and has high toxicity to the living organism. Some of the commercial dye reported as the causal factor of the skin irritation, dermatitis, allergy, and even cancer. Naturally, the dyes contaminated in the environment have high stability and not readily degraded[2].

The colored wastewater as the effluent of the textile industry process is one of the most dangerous environmental issues today. Its color will impart an aesthetic appearance in the water body, and moreover, it has high organic content which is not quickly degraded in the natural condition, high toxicity, mutagenicity, and carcinogenicity even in the low concentration state[3]. The contamination of dye in the wastewater hinders the passage of the light penetration into the water body, and the photosynthesis process will be disturbed[4]. Therefore, before being released to the environment the dye contamination on the industrial wastewater need to be treated.

e journal homepage www.jpacr.ub.ac.id
p-ISSN : 2302 – 4690 | e-ISSN : 2541 – 0733

This is an open access article distributed under the terms of the Creative Commons Attribution-NonCommercial 4.0 International which permits unrestricted use, distribution, and reproduction in any medium, provided the original work is properly cited. (http://creativecommons.org/licenses/by-nc/4.0/)

Many methods for dye removal from wastewater have been developed including membrane filtration, precipitation, coagulation, flocculation, chemical oxidation, solvent extraction, biodegradation, and adsorption[5–10]. However, in its application, the effectivity of these methods depends on many factors such as the dye chemical structure, the dependency on the pH condition, and the dye concentration in the wastewater. Among the developed methods, adsorption is considered as the most feasible way for the dye removal from wastewater in term of the flexibility of the operation process, efficiency, and maintenance cost[11].

The suitable adsorbents for dye removal have been widely studied in order to find the effective one. As reported by Calvete et. al.[12], activated carbon is one the most used adsorbent for dye and toxic pollutant in industrial scale due to its high surface area. However, the high cost of activated carbon preparation and the difficulties in the desorption process have restricted the use of activated carbon. Nowadays, many studies have been conducted in order to find an alternative cheap and suitable adsorbent to substitute the activated carbon utilization. Several types of low-cost adsorbent materials that have been developed including agricultural product, household wastes, industrial waste, sea materials, and clay materials[13].

Clay as the abundant natural materials is one of the most feasible low-cost adsorbents for dye removal due to the relatively high surface area and their well-developable structure. Many clays and clays minerals such as zeolite, smectite, kaolinite, sepiolite, and bentonite have widely employed as an adsorbent for dyes or heavy metals pollutant removal from wastewater. The high adsorption capability of the clay and clays mineral were affected by the total negative charge on the structure of the clay or clays mineral[13]. In the adsorption process, this negative charge will be neutralized by the positively charged adsorbate such as dye molecule or heavy metal ions.

Bentonite is the most widely utilized dioctahedral smectite mineral that mainly constructed by montmorillonite. The smectite mineral is the most important component of bentonite that arranged by 2:1 type of layer clay. It formed by two tetrahedral silica sheets (T) and an Alumina octahedral sheet (O). Naturally, the structure of bentonite is negatively charged due to the isomorphic substitution of Mg^{2+} for Al^{3+} in the octahedral sheet and Al^{3+} for Si^{4+} in the tetrahedral sheet. The negative charge of the bentonite structure is commonly balanced by the exchangeable cation such as Na^{+} and Ca^{+} that lied in the interlamellar space of the smectite [14].

Indonesia as one of the mineral-rich country has many natural bentonites deposit almost in every province[3]. Each bentonite deposit has their particular content composition that differs from the other deposit. Thus, their structural properties should be intensively investigated. The purpose of this work is to study the effect of natural and thermal activat bentonite from Sarolangun District of Jambi Province, Indonesia and to examine its ability as low-cost adsorbent material for removal of procion red dye from aqueous solution.

EXPERIMENT

Chemicals and instrumentation

The natural bentonite clay used in this work was grounded from Sarolangun District, Jambi Province, Indonesia. Prior to be utilized, the washing procedure of the natural bentonite was conducted to reduce the impurities content. The chemical composition of washed natural bentonite as oxide form was listed in **Table 1**. Procion Red MX-5B ($C_{19}H_{10}C_{l2}N_6Na_2O_7S_2$) with molecular weight 615.33 g mol^{-1} was obtained from Sigma-Aldrich without further purification. The procion red stock solution (1000 mg L^{-1}) was

prepared by dissolving 1 g procion red by 1 L distilled water. The procion red standard solution and working solution were prepared by diluting the procion red stock solution into the desired concentration using distilled water.

Table 1. Chemical properties of natural Sarolangun bentonite used in this study

Chemical composition	Concentration (%)
Al_2O_3	17.000
SiO_2	43.600
P_2O_5	0.710
K_2O	0.200
CaO	0.990
TiO_2	1.870
V_2O_5	0.110
Cr_2O_3	0.075
MnO	0.120
Fe_2O_3	33.390
NiO	0.887
CuO	0.150
ZnO	0.098

The thermal activation of natural bentonite was performed using Thermolyne muffle furnace from Thermo Scientific. The chemical structure of bentonite before and after the thermal activation process was conducted using Shimadzu X-Ray Diffractometer Lab-X type 6000 with scanning speed one deg min^{-1}. The functional group of the natural bentonite sample and the thermal activated sample was measured using FT-IR analysis using Shimadzu FT-IR Prestige-21 with KBr pellets the wavenumber 300-4000 cm^{-1}. The procion red concentration after the adsorption process was measured using UV-Visible spectrophotometer from Thermo Scientific type Genesys 20 at wavelength 530 nm.

Procedure reaction

Bentonite activation

The natural bentonite obtained from Sarolangun deposit of Jambi Province, Indonesia, was crushed and sieved to pass 200 mesh using ASTM standard sieve. The finely powdered bentonite then washed three times using distilled water to reduce the organic impurities than dried overnight in a laboratory oven at 105°C. The thermal activation of natural bentonite was conducted using a muffle furnace at a temperature 500°C for two hours. The sample then cooled and stored in a desiccator and ready to use as an adsorbent in procion red removal[15].

Adsorption Study

The adsorption studies to evaluate the capability of the thermal activated Indonesian bentonite for the removal of procion red dye from aqueous solution was carried out using the batch contact adsorption. The effect of the contact time, adsorbent dosage, initial dye concentration, initial pH solution, adsorption temperature, and adsorbent particle size on the adsorption of procion red were examined in a horizontal shaker with rotation speed 400 rpm. The fixed amount of thermal activated bentonite was added to a 250 mL erlenmeyer flask containing 50 mL of procion red solution. The solution then agitated for a specified time at various temperature. After adsorption, the mixture then separated by centrifugation for 5

minutes. The final concentration of the procion red after adsorption was measured using UV-Vis spectrophotometry at a maximum wavelength of procion red.

The amount of the procion red uptake and the percentage of the procion red removal were measured by the following equation.

$$q = \frac{(C_o - C_f)V}{m} \quad (1)$$

$$\%\ removal = \frac{(C_o - C_f)}{C_o}\ x\ 100 \quad (2)$$

Where q is the amount of procion red adsorbed (mg g^{-1}), C_o is the initial procion red concentration (mg L^{-1}), C_f is the final concentration of procion red after the adsorption process (mg L^{-1}). V is the volume of procion red solution used in the adsorption process (L), and m is the mass of the adsorbent used (g).

Adsorption Mechanism Study

The adsorption mechanism of procion red onto thermal activated bentonite adsorbent was studied based on the desorption study and instrument characterization of the adsorbent material before and the adsorption process. The desorption study of procion red was conducted in the batch system in order to evaluate the regeneration capability of thermal activated bentonite adsorbent. The desorption experiment was carried out according to the adsorption condition described in the previous section. At the end of the adsorption process, the dye contaminated adsorbent was separated and dried in the laboratory oven at 80°C for a night. The dried adsorbent then contacted with three types of eluent i.e. water (H_2O), sodium hydroxide (NaOH), and hydrochloric acid (HCl). The mixture then stirred in room temperature condition for 24 hours then separated using a centrifuge. After separation, the dye concentration in the eluent solution then measured by a spectrophotometer[16].

The adsorption mechanism study by instrument characterization was carried out under the same condition of the adsorption experiment in the previous section. After the adsorption process, the contaminated bentonite adsorbent then collected and dried in a laboratory oven at 80°C. The dry contaminated adsorbent then characterized using FT-IR and XRD. The obtained data then compared with the uncontaminated adsorbent.

RESULT AND DISCUSSION

Characterisation of The Adsorbent

FT-IR Analysis

The Fourier transform infrared (FT-IR) spectrometry analysis was conducted in order to evaluate the change of the natural bentonite before and after the thermal activation process. The FTIR spectrum of the natural bentonite (NB) and thermal activated bentonite (AB) shown in **Figure 1** and the description of the corresponding chemical bonds were described in **Table 2**. It can be seen in **Figure 1** that the main structure of the bentonite clay was observed as the bands of 470, 532, 910, and 1033 cm^{-1} [16].

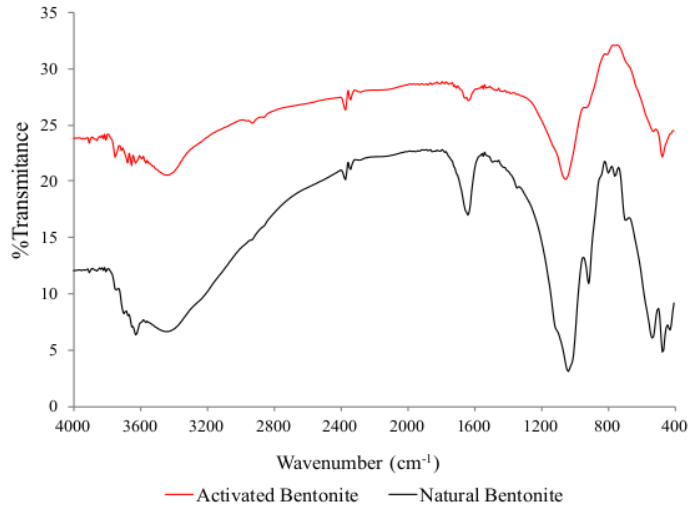

Figure 1. FT-IR Spectra of natural bentonite (NB) and thermal activated bentonite (AB)

The most noticeable difference from both spectrum lies in the particular band at the wavenumber around 1600 cm^{-1} and 3600 cm^{-1}. The peak of the activated bentonite (AB) at these wavenumbers was reduced dramatically compared to the natural bentonite indicate the change of the water content[17]. In the FTIR analysis, the water molecule commonly exhibits in the three kinds of vibration i.e. deformation of H-O-H group, symmetric, and asymmetric of O-H stretching. The reduce of the band around 1600 to 1700 cm^{-1} indicate the reduction of the H-O-H deformation group, while the decrease of the band around 3100 to 3700 cm^{-1} revealed the reducing of the O-H stretching group. These phenomena occurred due to the dihydroxylation process was triggered during the calcination process[18].

Table 2. The band of FTIR spectrum and corresponding chemical bonds for natural bentonite (NB) and activated bentonite (AB)

NB Bands	AB Bands	Chemical bonding
470	470	Si—O—Si deformation
532	-	Al—O—Si deformation
910	925	Si—O stretching
1033	1049	Si—O stretching
1635	1635	O—H deformation of water
3448	3448	H—O—H stretching
3626	3749	O—H stretching (hydroxyl group)

Table 3. Interlayer spacing and FWHM value of natural and activated bentonite

Adsorbent	2 theta	*d* (001)	FWHM
Natural bentonite	5.0337	17.5414	1.5675
Activated bentonite	6.1339	14.3973	0.1021

XRD Analysis

The XRD powder patterns of bentonite and thermal activated bentonite at various temperatures were illustrated in **Figure 2**. Natural bentonite has main characteristic patterns of montmorillonite at 2θ about 5°. Natural bentonite also contains montmorillonite at 2θ of about 20° and 26°, illite at 2θ of about 19°, and quartz at 2θ of about 39°[19]. According to Chen et al.,[20] bentonite is one of the montmorillonite-smectite group minerals thus natural bentonite contains mixtures all these minerals. Thermal activation of bentonite was conducted systematically under oxygen atmospheric conditions at 500°C before used as an adsorbent. The XRD powder patterns of bentonite after thermal activation showed that montmorillonite fraction was reduced significantly at 2θ of around 5° as presented in **Figure 11**. Moreover, as listed in **Table 3**, the interlayer spacing and FWHM value of activated bentonite decreased compared to natural bentonite. This result is indicating the removal of a water molecule between the crystal lattice sheet and the distortions in crystalline structure caused by high temperature during the thermal activation process[16].

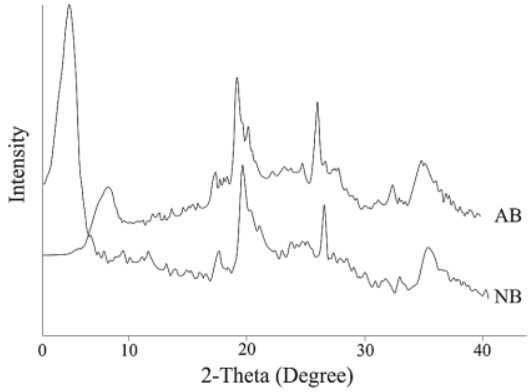

Figure 2. XRD pattern of natural bentonite (NB) and activated bentonite (AB)

TG-DTA Analysis

The thermogravimetric curve (TGA) that represent the mass of the sample material in relation to the heating rate and the differential thermal (DTA) curve of the natural and activated bentonite sample was depicted in **Figure 3**. For the natural bentonite sample, two endothermic peaks were observed. The first endothermic peak was clearly identified in the temperature range between 30–120°C. These peaks assigned 12% mass loss of water[21]. The second endothermic peak was in the range of temperature between 450–470°C, which was related with dihydroxylation of bentonite and also rearrangements of the silica-alumina framework on natural bentonite due to loss of water[22]. For the activated bentonite sample, only one endothermic peak was identified at temperature range 30–120°C similar with natural bentonite, which was attributed to 3% mass loss of water[22]. The TG profile of the activated bentonite showed that activation of bentonite at 500°C did not affect into silica-alumina framework structure on bentonite.

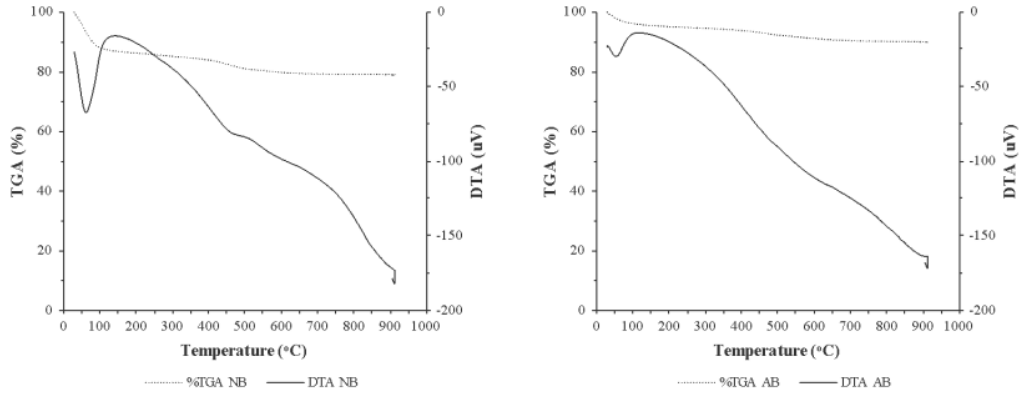

Figure 3. TGA and DTA profile of natural bentonite (NB) and activated bentonite (AB)

Procion Red Adsorption Study

Effect of pH Condition

The adsorption process is profoundly affected by the pH condition as the most important factor. At the same time, the pH condition can affect the ionization degree of the adsorbate functional group, the adsorbent surface charges, and even the adsorption mechanism. In order to study the effect of the procion red uptake to the natural and activated bentonite, in this work, the experiment was conducted by varying the initial pH condition ranging from 3 to 11 at the constant dye concentration and defined adsorption time. **Figure 4**, represents the effect of initial pH condition to the dye removal percentage. The result shows that the maximum dye removal observed occurred at relatively acidic condition (pH value around 4). At the basis solution condition, the dye removal was decreased significantly. This result can be simply explained that in the alkaline condition, hydroxyl ions on the adsorbent surface is excessive. Since the procion red was an anionic dye, the exceed of hydroxyl ions will compete with the dye to be uptaken into the adsorbent surface[23].

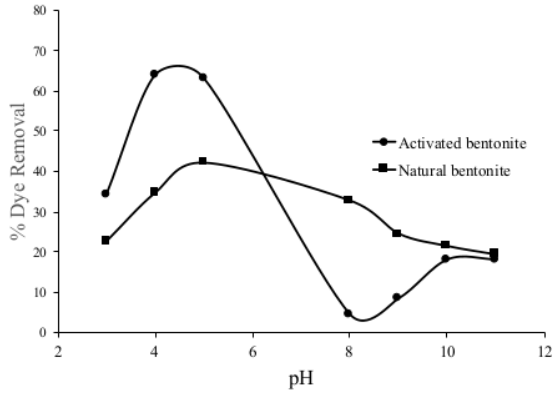

Figure 4. Effect of initial pH on the adsorption of procion red onto natural and thermal activated bentonite

Effect of Contact Time

The effect contact time was investigated by contacting bentonite with the procion red as a function of time in the range of 10–120 min at a constant procion red concentration (10 mg L^{-1}) and temperature. The results of procion red adsorption onto natural and thermal activated bentonite are provided in **Figure 5**. As can be seen in the figure, the adsorption capacity of the procion red onto thermal activated bentonite was greater than to the natural bentonite. Moreover, the procion red uptake to the thermal activated bentonite is rapidly reached the maximum adsorption capacity almost in the first 10 minutes of contact time. However, the procion red uptake to the natural bentonite is running slowly to reach the maximum adsorption capacity and equilibrium state. The maximum adsorption capacity of the procion red onto natural bentonite reached after almost 90 minutes of contact time. As reported by Kulkarni et al.[4], the higher velocity of the dye uptake onto thermal activated bentonite indicate that the thermal activated bentonite has better availability of larger surface area.

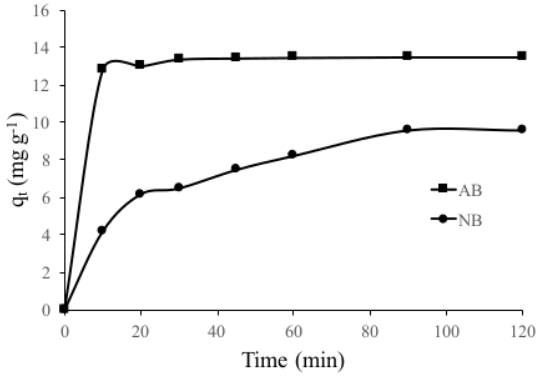

Figure 5. Effect of contact time on the procion red adsorption onto natural bentonite (NB) and activated bentonite (AB)

Effect of Initial Procion Red Concentration

In order to study the effect of initial concentration to the adsorption capacity of natural and activated bentonite, the adsorption experiments were conducted at the different initial procion red concentration in the range of 2–80 mg L^{-1}. The result of this study was shown in **Figure 6** as the plot of initial dye concentration against the adsorption capacity (q_e). **Figure 6** indicates that by increasing the initial dye concentration, the amount of dye adsorbed gradually increases both to the natural bentonite and activated bentonite. The procion red uptake to the natural bentonite increase from 0.2 to 4.3 mg g^{-1} by increasing the initial dye concentration from 2 to 80 mg L^{-1}. Procion red uptake has higher adsorption capacity increasing from 1.4 to 7.1 mg g^{-1} by increasing the initial dye concentration from 10 to 80 mg L^{-1} into the activated bentonite. The increasing of the adsorption capacity due to the increase of the initial concentration affecting the enhance of the driving force to the mass transfer between the adsorbent and the adsorbate[24].

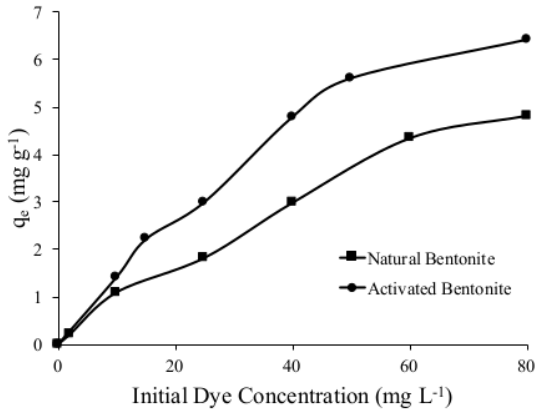

Figure 6. Effect of initial dye concentration on the adsorption of procion red onto natural and activated bentonite

Adsorption Kinetic Study

Adsorption kinetic study is one of the most important criteria to measure the adsorption efficiency of an adsorbent. Moreover, the adsorption mechanism can be considered from the result of the kinetic data. In this work, three adsorption kinetic models were applied in order to analyze the possibility of the adsorption model of the procion red onto activated bentonite i.e. pseudo-first order, pseudo-second order, and intra-particle diffusion. The pseudo-first order model as a simple kinetic analysis is expressed as the following equation.

$$\log(q_t - q_e) = \log q_e - \frac{k_1}{2.303} t \qquad (3)$$

Where q_t and q_e are the amount of the dye adsorbed at the time t and at the equilibrium state (mg g^{-1}), respectively. k_1 represents the pseudo-first order rate constant (min^{-1}) and t is the adsorption time (min). In order to evaluate the value of the coefficient of k_1 and q_e, the linear plot between log(q_t-q_e) and t was made and the values of k_1 and q_e determined as the slope and intercept of the linear equation produced.

Table 4. Pseudo-first and second order kinetic coefficient

Adsorbent	Pseudo-first order			Pseudo-second order		
	q_e (mg g^{-1})	k_1 (min^{-1})	R^2	q_e (mg g^{-1})	k_2 (g mg^{-1} min^{-1})	R^2
Natural bentonite	6.41	0.002	0.8118	11.086	0.0048	0.99424
Activated bentonite	73.63	0.594	0.9774	13.568	0.1272	0.99999

The pseudo-second-order kinetic model was applied base on the adsorption equilibrium capacity expressed by the following equation:

$$\frac{t}{q_t} = \frac{1}{k_2 q_e^2} + \frac{1}{q_e} t \qquad (4)$$

Where t is the adsorption time (min), q_t and q_e are the amount of the dye adsorbed at time t and the equilibrium state (mg g^{-1}), respectively. k_2 is the pseudo-second order rate constant. The kinetic coefficient of q_e and k_2 was calculated from the slope and intercept of the linear equation by plotting the t/q_t against t.

The plot of first and second-order kinetic model, the obtained parameter data, and the correlation coefficient are given in **Figure 7** and **Table 4**. Based on the result depicted in **Figure 7**, both the kinetic models seem fit enough to describe the adsorption dynamic in all adsorbent used with high coefficient correlation. However, in more detail, the pseudo-second order model appears to be more adapted. The R^2 value of the second-order model for natural and activated bentonite are 0.99424 and 0.99999, respectively. These values are higher than the pseudo-second order model with the R^2 value 0.8118 and 0.9774 for natural bentonite and activated bentonite, respectively.

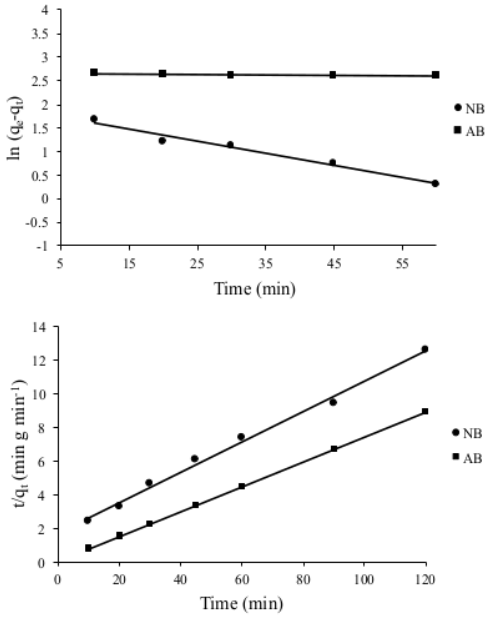

Figure 7. First-order kinetic models (A) and second-order kinetic model (B) plot of procion red onto natural bentonite (NB) and activated bentonite (AB)

Adsorption Isotherm Study

The study of the adsorption isotherm is a useful method to indicate the distribution of the molecule between the solid and liquid phase when the adsorption process reaches the equilibrium. The fit model for the adsorption designing purpose can be analyzed by fitting the isotherm data to the different isotherm models. Recently, many isotherm equation models have been developed in order to analyze the experimental adsorption equilibrium data. In this work, the isotherm data were analyzed by two common isotherm equation models, Langmuir and Freundlich isotherm model. These two isotherm equations are as follows:

Langmuir adsorption isotherm model

Langmuir isotherm model is based on the monolayer adsorption that the adsorption process occurs in the uniform site. The equation of the Langmuir isotherm model is listed below [25]:

$$\frac{1}{q_e} = \frac{1}{q_m} + \frac{1}{q_m K_L}\left(\frac{1}{C_e}\right) \qquad (5)$$

Where q_e denotes the concentration of the dye adsorbed per unit mass of the adsorbent (mg g^{-1}), q_m is the Langmuir constant based on the maximum adsorption capacity (mg g^{-1}), and K_L is Langmuir constant based on the energy constant of the adsorption capacity (L mg^{-1}), C_e is the dye concentration at the equilibrium state (mg L^{-1}).

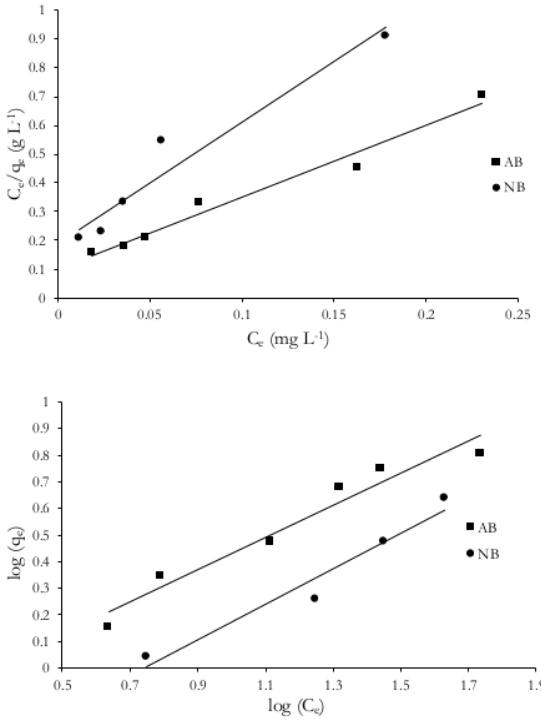

Figure 8. Plot of Langmuir (A) and Freundlich (B) for adsorption of procion red by natural bentonite (NB) and activated bentonite (AB)

Table 5. Langmuir and Freundlich adsorption isotherm parameter

Adsorbent	Langmuir isotherm			Freundlich isotherm		
	K_L (mg g^{-1})	q_m (mg g^{-1})	R^2	K_F (mg g^{-1})	n	R^2
Natural bentonite	0.0450	5.26	0.9422	0.3205	1.49	0.9544
Activated bentonite	0.0400	9.97	0.9730	0.6669	1.64	0.9498

Freundlich adsorption isotherm model

The Freundlich isotherm model is one of the most applied models in order to describe the adsorption equilibrium. This model explains that in the solid-liquid adsorption phase, the different site of the adsorbent has a different adsorption energy involved during the adsorption process. Further, this model describes the relation both the amount of dye adsorbed per mass unit and the equilibrium concentration of the similar dye. Freundlich isotherm model as described in the following equation:

$$logq_e = logK_F + \left(\frac{1}{n}\right)logC_e \qquad (6)$$

Where K_F is Freundlich isotherm constant indicates the adsorption capacity and n is the Freundlich constant indicates the adsorption intensity[26]. The result of the plot of Langmuir and Freundlich adsorption isotherm model is shown in **Figure 8**. The correlation values (R^2) for the Langmuir and Freundlich isotherm model for both natural and activated bentonite adsorbent is presented in **Table 5**. The obtained results showed that both types of adsorbents have different tendencies toward the isotherm model used. Procion red adsorption onto natural bentonite is well described by Freundlich isotherm model, while the procion red adsorption onto activated bentonite seems more appropriate to simulated by Langmuir isotherm model. Moreover, the Langmuir capacity (q_m) of the activated bentonite has a higher value than the natural bentonite. As described in table 4, K_F value of natural bentonite is 0.32, whereas K_F value of activated bentonite is 0.66. It was indicated that the procion red adsorption is more favorable in the activated bentonite adsorbent and the activated bentonite has higher adsorption affinity toward procion red dye.

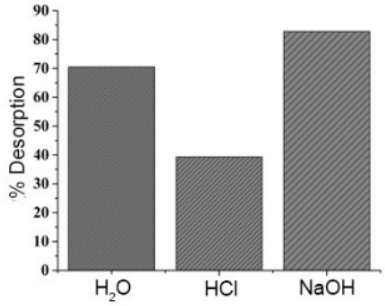

Figure 9. Percent desorption of the adsorbed procion red into the various eluent

Adsorption Mechanism Study

The adsorption mechanism of procion red onto bentonite mechanism was investigated by desorption, spectroscopic, and diffraction studies. The desorption study was carried out using water, hydrochloric acid, and sodium hydroxide as eluent sequentially in separate batch systems. **Figure 9** shows the desorption of the adsorbed dye in each eluent. The results indicated that sodium hydroxide and water could desorb procion red higher than hydrochloric acid. It means that oxygen from water and a hydroxyl group from sodium hydroxide play a significant role in the bentonite-procion red interactions. This assumption is equivalent to the results of spectroscopic measurement using FTIR as shown in **Figure 10**. The band at 1630 cm^{-1} was split into two bands at 1636 cm^{-1} and 1528 cm^{-1}. This band attributed O-H deformation of bentonite bond with procion red. The bands at 3430 cm^{-1} and 3620 cm^{-1} also showed broad peak due to strong interaction adsorbate with adsorbent[27-28].

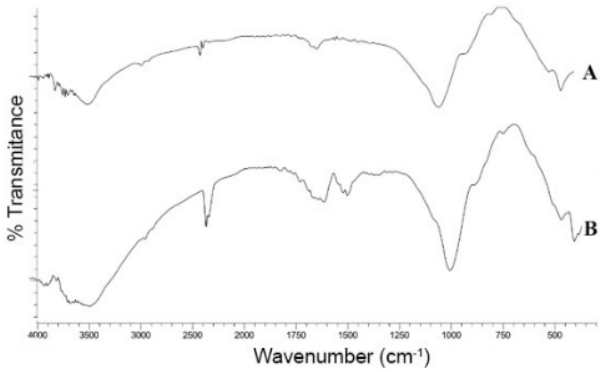

Figure 10. FTIR spectra for activated bentonite (A) and procion red contacted bentonite (B)

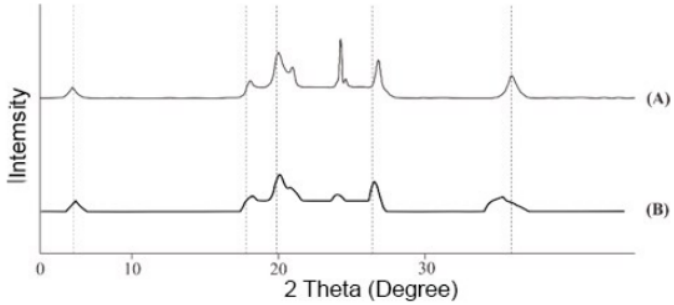

Figure 11. XRD pattern of activated bentonite (A) and procion red contacted bentonite

XRD powder pattern (**Figure 11**) also indicated procion red bond to bentonite via montmorillonite as active sites. The peak of montmorillonite on activated bentonite at 26° was shifted into 28° after bind with procion red together with decreasing of intensity peak. Probably the procion red bond with hydroxyl group as active sites in montmorillonite strongly than bond with oxygen and another species group on bentonite[29]. Following the above results and others studies, adsorption of procion red on bentonite occurred between oxygens of bentonite as active sites and dichlorotriazine species from procion red. We proposed adsorption reaction mechanism as presented in **Figure 12**.

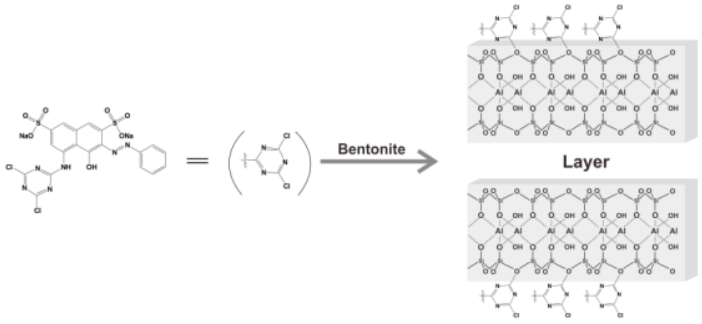

Figure 12. Plausible adsorption mechanism of procion red onto activated bentonite

CONCLUSION

In summary, the simple modification of Sarolangun bentonite by thermal activation at 500°C has successfully improved the adsorption behavior of natural bentonite toward procion red dye. Moreover, the activation process did not significantly change the structure of the natural bentonite host. The batch adsorption experiment by comparing the natural bentonite and activated bentonite showed that the adsorption process by activated bentonite was highly efficient in the relatively acidic pH condition and quick contact time. The kinetic study of the procion red adsorption toward activated bentonite follows the pseudo-second-order kinetic model and the adsorption isotherm study reveals that the best fit for the equilibrium data was followed the Langmuir isotherm.

ACKNOWLEDGMENT

The authors are thankful to Kementerian Riset dan Pendidikan Tinggi (Kemenristekdikti) Republik Indonesia for financially supporting this research through Program Magister Menuju Doktor Untuk Sarjana Unggul (PMDSU) Batch II Grant with contract number 468/UN9.3.1/LT/2017 and 326/SP2H/LT/DRPM/IX/2016.

REFERENCES

[1] Das, D., Karan, C. K., Bhattacharjee, M. *Polyhedron* **2017**, *124*, 51–61.
[2] Stawiński, W., Węgrzyn, A., Dańko, T., Freitas, O., Figueiredo, S., Chmielarz, L. *Chemosphere* **2017**, *173*, 107–115.
[3] Taher, T., Mohadi, R., Rohendi, D., Lesbani, A. In *AIP Conference Proceedings*, 2017, p 20028.
[4] Kulkarni, M. R., Revanth, T., Acharya, A., Bhat, P. *Resour. Technol.* **2017**, *3* (1), 71–77.
[5] Karagüzel, C., Çetinel, T., Boylu, F., Çinku, K., Çelik, M. S. *Appl. Clay Sci.* **2010**, *48* (3), 398–404.
[6] Hairom, N. H. H., Mohammad, A. W., Kadhum, A. A. H. *J. Water Process Eng.* **2014**, *4*, 99–106.
[7] Zhu, M.-X., Lee, L., Wang, H.-H., Wang, Z. *J. Hazard. Mater.* **2007**, *149* (3), 735–741.
[8] Szyguła, A., Guibal, E., Ruiz, M., Sastre, A. M. *Colloids Surfaces A Physicochem. Eng. Asp.* **2008**, *330* (2–3), 219–226.
[9] Habiba, U., Siddique, T. A., Joo, T. C., Salleh, A., Ang, B. C., Afifi, A. M. *Carbohydr. Polym.* **2017**, *157*, 1568–1576.
[10] Rahman, A., Urabe, T., Kishimoto, N. *Procedia Environ. Sci.* **2013**, *17*, 270–278.
[11] Goswami, M., Phukan, P. *J. Environ. Chem. Eng.* **2017**, *5* (4), 3508–3517.
[12] Calvete, T., Lima, E. C., Cardoso, N. F., Dias, S. L. P., Pavan, F. A. *Chem. Eng. J.* **2009**, *155* (3), 627–636.
[13] Ali, I., Asim, M., Khan, T. A. *J. Environ. Manage.* **2012**, *113*, 170–183.
[14] Erdoğan Alver, B., Alver, Ö. *Spectrochim. Acta - Part A Mol. Biomol. Spectrosc.* **2012**, *94*, 331–333.
[15] Toor, M., Jin, B., Dai, S., Vimonses, V. *J. Ind. Eng. Chem.* **2015**, *21*, 653–661.
[16] Cantuaria, M. L., De Almeida Neto, A. F., Nascimento, E. S., Vieira, M. G. A. *J. Clean. Prod.* **2016**, *112*, 1112–1121.
[17] Ait Sidhoum, D., Socías-Viciana, M. M., Ureña-Amate, M. D., Derdour, A., González-Pradas, E., Debbagh-Boutarbouch, N. *Appl. Clay Sci.* **2013**, *83–84*, 441–448.
[18] Bertagnolli, C., Kleinübing, S. J., Gurgel, M. *Appl. Clay Sci.* **2011**, *53* (1), 73–79.

[19] Terzić, A., Pezo, L., Andrić, L., Pavlović, V. B., Mitić, V. V. *Ceram. Int.* **2017**, *43* (2), 2549–2562.
[20] Chen, Y., Zhu, C., Sun, Y., Duan, H., Ye, W., Wu, D. *J. Radioanal. Nucl. Chem.* **2012**, *292* (3), 1339–1347.
[21] Belbachir, I., Makhoukhi, B. *J. Taiwan Inst. Chem. Eng.* **2017**, *75*, 105–111.
[22] Caglar, B., Afsin, B., Tabak, A., Eren, E. *Chem. Eng. J.* **2009**, *149* (1–3), 242–248.
[23] Subramani, S. E., Thinakaran, N. *Process Saf. Environ. Prot.* **2017**, *106*, 1–10.
[24] Belbachir, I., Makhoukhi, B. *J. Taiwan Inst. Chem. Eng.* **2016**, *75*, 105–111.
[25] Mishra, S. R., Chandra, R., Kaila A., J., Darshi B., S. *Environ. Technol. Innov.* **2017**, *7*, 87–101.
[26] Aytas, S., Yurtlu, M., Donat, R. *J. Hazard. Mater.* **2009**, *172* (2–3), 667–674.
[27] Yaming, L., Mingliang, B., Zhipeng, W., Run, L., Keliang, S., Wangsuo, W. *J. Taiwan Inst. Chem. Eng.* **2016**, *62*, 104–111.
[28] Kordouli, E., Bourikas, K., Lycourghiotis, A., Kordulis, C. *Catal. Today* **2015**, *252*, 128–135.
[29] Kalmár, J., Lente, G., Fábián, I. *Dye. Pigment.* **2016**, *127*, 170–178.

View publication stats

C.4b.1-JPACR2018.pdf

ORIGINALITY REPORT

11%
SIMILARITY INDEX

PRIMARY SOURCES

1	www.researchgate.net Internet	183 words —	4%
2	www.mdpi.com Internet	78 words —	2%
3	www.ojs.pps.unsri.ac.id Internet	65 words —	1%
4	eprints.unsri.ac.id Internet	63 words —	1%
5	www.intechopen.com Internet	39 words —	1%
6	www.smujo.id Internet	31 words —	1%
7	www.coursehero.com Internet	28 words —	1%
8	iwaponline.com Internet	27 words —	1%
9	www.ijcps.org Internet	27 words —	1%
10	www.aidic.it Internet		

26 words — 1%

EXCLUDE QUOTES	OFF	EXCLUDE MATCHES	< 1%
EXCLUDE BIBLIOGRAPHY	ON		